Published by :
http://www.ijert.org

International Journal of Engineering Research & Technology (IJERT)
ISSN: 2278-0181
Vol. 6 Issue 02, February-2017

Design of GPS Compass for Lightweight UAVs

Wei Dou, Ganning Fu,Wantong Chen
School of Electronics Information and Automation
Civil Aviation University of China
Tianjin, China

***Abstract*—Satellite compasses equipped with short baselines can provide precise heading and elevation information for various vehicles. Compared with the magnetic compass, the heading determination of satellite compass doesn't depend on latitude, velocity and the Earth's magnetic field, with the advantage of driftless. The design of this contribution aims to provide a satellite compass prototype system for lightweight UAVs, and the implementation is verified to be very light, small, high accuracy, high rates and long-endurance. The core algorithm is to use the C-LAMBDA algorithm, and the hardware platform is based on the core board with Cortex-A8 architecture and the UBLOX LEA-6T satellite navigation chip, and final true heading results will be sent to the terminals via a Bluetooth link.**

Keywords—GPS compass; lightweight UAV; short baseline; integer ambiguity resolution; true heading

I. INTRODUCTION

In the past five decades, the magnetic compass is often utilized for heading determination of unmanned aerial vehicle (UAV). The magnetic compass contains a magnet that interacts with the earth's magnetic field and aligns itself to point to the magnetic poles. However, the accuracy of the magnetic compass is affected by the magnetic field intensity nearby the equipment, and it suffers from various errors.

In recent years, there is a growing interest in GPS (Global Positioning System) compass system. For this technique, one antenna is assumed to be a reference and another is assumed to be a rover. By finding the baseline vector defined by two antennas, one is able to estimate the pointing direction, namely the compass solution. Compared with the magnetic compass, the GPS compass does not depend on the magnetic field, the moving velocity and the latitude [2].

To obtain the high-precision heading and elevation, the precise carrier phase measurements from two antennas and an integer ambiguity resolution method are used to obtain precise yaw and pitch in this system [3]. Integer ambiguity resolution (IAR) is the process of resolving the unknown cycle ambiguities of the carrier phase data as integer, and many studies have been carried out to investigate the IAR method. More recent IAR methods make use of the Constrained LAMBDA (CLAMBDA) method to estimate the integer ambiguity, which is proved to be a fast, reliable estimator [4]. With this estimator, the successful ambiguity resolution can be achieved by utilizing instantaneous measurements, namely the single epoch ambiguity resolution, thus making IAR a total independence from carrier phase slips and losses of lock [5].

This work is supported by the Undergraduate Training Programs for Innovation and Entrepreneurship of Civil Aviation University of China (Grant No.IECAUC2016132).

As a new type of compass, the correctness of resolved heading and elevation should be verified for UAVs. The design of this contribution aims to provide a satellite compass prototype system for UAV platforms. Thus, we focus the following characteristics: light, small, high accuracy, high rates and long-endurance. The final implementation is verified on the six-rotor UAV.

II. THE THEORETICAL MODEL OF GPS COMPASS

A. Yaw and Pitch Estimation

For GPS compass equipped with a short baseline $\boldsymbol{b}$, the yaw and pitch of the UAV can thus be computed. If the baseline vector from reference antenna to another antenna is parameterized with respect to the local East-North-Up frame, the heading ψ and the elevation θ can be computed from the baseline components (coordinates) b_E, b_N and b_U as

$$\psi = \tan^{-1}\left(b_E / b_N\right) \tag{1}$$

$$\theta = \tan^{-1}\left(b_U \Big/ \sqrt{b_N^2 + b_E^2}\right) \tag{2}$$

B. GPS Compass Mathmatical Model

With a prior baseline length l, the mathematical model of GPS compass reads as [6]:

$$E(\boldsymbol{y}) = \boldsymbol{A}\boldsymbol{a} + \boldsymbol{B}\boldsymbol{b}, D(\boldsymbol{y}) = \boldsymbol{Q}_y, \boldsymbol{a} \in Z^n, \boldsymbol{b} \in R^3, \|\boldsymbol{b}\| = l \tag{3}$$

where $\boldsymbol{y}$ is the given GPS data vector, and $\boldsymbol{a}$ and $\boldsymbol{b}$ are the ambiguity vector and the baseline vector of order n and 3 respectively. $E(\cdot)$ and $D(\cdot)$ denote the expectation and dispersion operators, respectively, and $\boldsymbol{A}$ and $\boldsymbol{B}$ are the given design matrices that link the data vector to the unknown parameters. The variance matrix of $\boldsymbol{y}$ is given by the positive definite matrix $\boldsymbol{Q}_y$, which fully characterizes the statistical properties of the given GNSS data vector. Since the baseline length is often known in practical applications, this priori given baseline information can be treated as a useful constraint as well. In Equation (3), l denotes the known baseline length, which is assumed to be constant. Note that the GPS compass model (3) involves two types of constraints: the integer constraints on the ambiguities and the length constraint on the baseline vector. For this model, once $\boldsymbol{a}$ is resolved, the least-squares solution for $\boldsymbol{b}$, namely the conditional least-squares solution, can be written as

$$\hat{\boldsymbol{b}}(\boldsymbol{a}) = \left(\boldsymbol{B}^T \boldsymbol{Q}_y^{-1} \boldsymbol{B}\right)^{-1} \boldsymbol{B}^T \boldsymbol{Q}_y^{-1} (\boldsymbol{y} - \boldsymbol{A}\boldsymbol{a}) \tag{4}$$

The corresponding variance matrix is given as

$$\boldsymbol{Q}_{\hat{\boldsymbol{b}}(\boldsymbol{a})} = \left(\boldsymbol{B}^T \boldsymbol{Q}_y^{-1} \boldsymbol{B}\right)^{-1} \tag{5}$$

International Journal of Engineering Research & Technology (IJERT)
ISSN: 2278-0181
Vol. 6 Issue 02, February-2017

To solve the GPS model (3), one usually applies the least-squares principle and this amounts to solving the following minimization problem:

$$\min_{\boldsymbol{a}\in Z^n,\boldsymbol{b}\in R^3,\|\boldsymbol{b}\|=l} \|\boldsymbol{y}-\boldsymbol{A}\boldsymbol{a}-\boldsymbol{B}\boldsymbol{b}\|^2_{Q_y} \quad (6)$$
$$= \|\hat{\boldsymbol{e}}\|^2_{Q_y} + \min_{\boldsymbol{a}\in Z^n}\left(\|\hat{\boldsymbol{a}}-\boldsymbol{a}\|^2_{Q_{\hat{a}}} + \min_{\boldsymbol{b}\in R^3,\|\boldsymbol{b}\|=l}\|\hat{\boldsymbol{b}}(\boldsymbol{a})-\boldsymbol{b}\|^2_{Q_{\hat{b}(a)}}\right)$$

where $\|(\cdot)\|^2_{Q_y} = (\cdot)^T \boldsymbol{Q}_y^{-1}(\cdot)$ and $\hat{\boldsymbol{e}}$ is the least squares residuals. Moreover, the following cost function can be formulated [7]:

$$\min_{\boldsymbol{a}\in Z^n}\left(\|\hat{\boldsymbol{a}}-\boldsymbol{a}\|^2_{Q_{\hat{a}}} + \min_{\boldsymbol{b}\in R^3,\|\boldsymbol{b}\|=l}\|\hat{\boldsymbol{b}}(\boldsymbol{a})-\boldsymbol{b}\|^2_{Q_{\hat{b}(a)}}\right) \quad (7)$$

In this case, the conditional least-squares solution for $\boldsymbol{b}$ and its variance matrix are both required for the estimator. The solution to the minimization problem follows therefore as

$$\breve{\boldsymbol{a}} = arg\min_{\boldsymbol{a}\in Z^n}\left(\|\hat{\boldsymbol{a}}-\boldsymbol{a}\|^2_{Q_{\hat{a}}} + \min_{\boldsymbol{b}\in R^3,\|\boldsymbol{b}\|=l}\|\hat{\boldsymbol{b}}(\boldsymbol{a})-\boldsymbol{b}\|^2_{Q_{\hat{b}(a)}}\right) \quad (8)$$
$$\breve{\boldsymbol{b}} = \hat{\boldsymbol{b}}(\breve{\boldsymbol{a}})$$

This can be solved by the Constrained (C-) LAMBDA method with high efficiency and high success rate [8].

C. *Accuracy of GPS Compass*

The baseline vector in the local East-North-Up frame can be expressed as follows:

$$\boldsymbol{b} = \begin{bmatrix} b_E \\ b_N \\ b_U \end{bmatrix} = \begin{bmatrix} l\sin\psi\cos\theta \\ l\cos\psi\cos\theta \\ l\sin\theta \end{bmatrix} \quad (9)$$

With σ_E^2, σ_N^2 and σ_U^2 being the variances of b_E, b_N and b_U, the yaw and pitch accuracy of GPS compass can be written as [9]:

$$\sigma^2_{\delta\psi} = \frac{(\cos\psi)^2\sigma_E^2 + (\sin\psi)^2\sigma_N^2}{l^2(\cos\theta)^2} \quad (10)$$

$$\sigma^2_{\delta\theta} = \frac{(\sin\psi\sin\theta)^2\sigma_E^2 + (\cos\psi\sin\theta)^2\sigma_N^2 + (\cos\theta)^2\sigma_U^2}{l^2} \quad (11)$$

The equations above show that the accuracies of the estimated yaw and pitch are inverse proportional to the length of the baseline used. Thus, for longer baseline, the accuracy of the GPS compass is higher.

III. STRUCTURAL DESIGN OF GPS COMPASS FOR SIX-ROTOR UAV

With the discussion on the mathematical model and the accuracy assessment of GPS compass, a structural design is proposed for the lightweight six-rotor UAV.

A. *The Patch Antennas*

Patch antennas are ideal for the UAV application where the lightweight antenna is required. Ceramic patch antennas are very popular because of their small size, typically measuring 25 x 25 mm^2 down to 10x10 mm^2. The performance of a patch antenna heavily depends on the size, shape and symmetry of the ground plane. In this contribution, three typically 25 x 25 mm^2 ceramic patch antennas are utilized, see Fig.1and Fig.2.

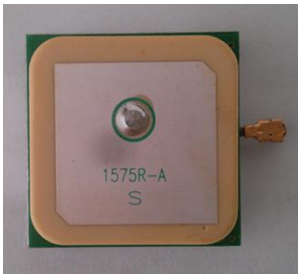

Fig.1 Typically 25 x 25 mm^2 ceramic patch antenna

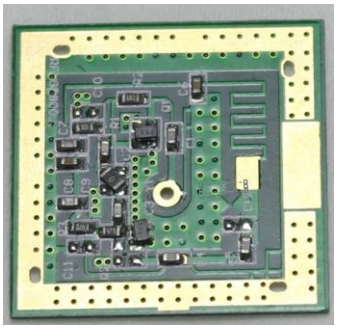

Fig.2 The PCB design of ceramic patch antenna

B. *The Baseline Placement*

Three ceramic patch antennas can form double collinear baselines but with distinctly different lengths. In order to improve the reliability, both baselines are setup in the collinear way. In other words, three antennas are employed and set up in the same straight line, which is shown in Fig.3.

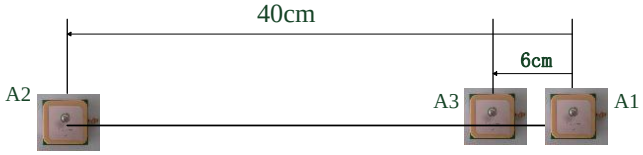

Fig.3 Double collinear baselines with three antennas

The first baseline is setup with Antenna 1 and Antenna 2 in Fig.1, and the second baseline is setup with Antenna 3 and Antenna 2. If the first baseline is resolved to be consistent with the second baseline, the resolved baseline is treated as correct.

C. *The GPS Receivers*

To implement a satellite compass prototype system for UAVs, the lightweight GPS receivers with raw carrier phase measurements must be utilized.

In order to implement it with low cost, three U-Blox LEA-6T receivers are utilized for hardware platform. The U-Blox LEA-6T receiver has the raw measurements including carrier phase and code. It is widely used for time service and attitude determination, with a high cost performance. For LEA-6T module, the hardware integration work should be carefully achieved for best performance. The LEA-6T module and the single receiver hardware board are demonstrated in Fig.4.

International Journal of Engineering Research & Technology (IJERT)
ISSN: 2278-0181
Vol. 6 Issue 02, February-2017

Fig.4 LEA-6T module and the GPS receiver hardware board

D. IMU and Processor

The rate of raw measurements of LEA-6T is up to 5Hz. However, for UAV applications, this is not enough. In order to improve the output rate of true heading, the MPU6050 module is integrated in the GPS compass system. The MPU6050 is the world's first integrated 6-axis motion tracking device that combines a 3-axis gyroscope, 3-axis accelerometer, and a digital motion processor, see Fig.5. The MPU6050 module provides instrumentation grade performance and measuring ranges ±90° with a 0.1° digital output resolution. Dual axis inclination measurements (X and Y) will provide an aid for the GPS compass system and only the X-axis measurement is used for GPS compass system. Low temperature dependency, high resolution and low noise, together with low cost design, make the MPU6050 the ideal choice.

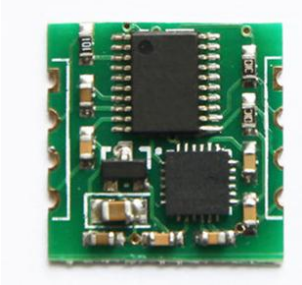

Fig.5 The MPU6050 module

All the raw measurements of LEA-6T receivers and MPU6050 are processed by ARM Cortex-A8 processor (S5PV210) and for convenience the raw data and final results are broadcasted by Wireless Bluetooth High Speed Adapter. Fig.6 demonstrates the appearance of PCB design based on the Samsung S5PV210 chip.

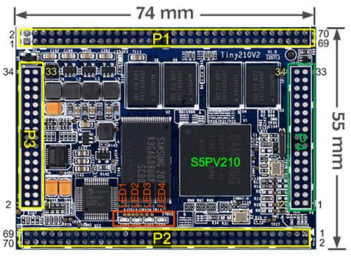

Fig.6 Cortex-A8 processor

E. The Prototype System for UAV

In order to analyze the principle of GPS compass for six-rotor UAV, we use solidworks software for modeling and use 3D-printer to form the mechanical structure. The prototype system of the compass with double baseline is determined in Fig.7. The weight of the whole prototype system is only about 400g, which is light enough for UAV application.

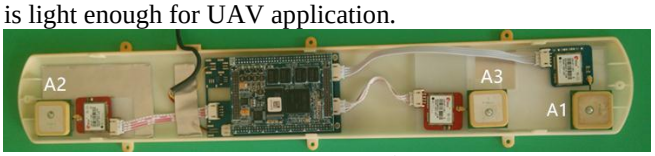

Fig.7 The prototype system for UAV

We have implemented our method with C language and applied them to the real-time measurements from prototype system with 20 Hz output. All the raw measurements of LEA-6T receivers and MPU6050 are processed together by ARM Cortex-A8 processor. For the real-time application, current GPS measurements must be combined with the latest measurement of the MPU6050. Note that high rate measurements can help reduce the synchronization error.

IV. EXPERIMENTS

This section presents the evaluation of the prototype system based on actual six-rotor UAV. The accuracy of yaw is also evaluated.

A. Six-rotor UAV Test Platform

One six-rotor UAV is used as the test platform. The GPS compass prototype system is mounted on the top of UAV, see Fig.8.

Fig.8 The six-rotor UAV test platform

The proposed method has been tested processing actual data collected during a dynamic experiment, in which the UAV is moving towards west. During about 1000 seconds observation, the number of available satellites equals seven or six most of the time. The numbers of visible satellites are given in Fig.9.

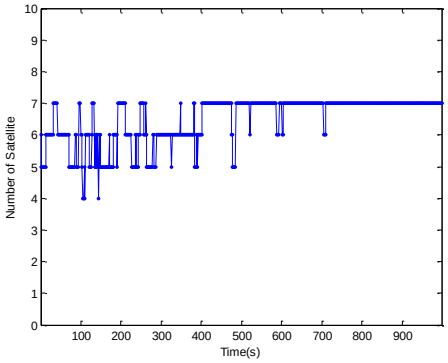

Fig.9 The number of visible satellites

International Journal of Engineering Research & Technology (IJERT)
ISSN: 2278-0181
Vol. 6 Issue 02, February-2017

B. Heading Determination

The heading/yaw and elevation/pitch are resolved based on the model (8) with Constrained (C-) LAMBDA method. In order to suppress the vibration noise, the yaw results are filtered with a Kalman filter.

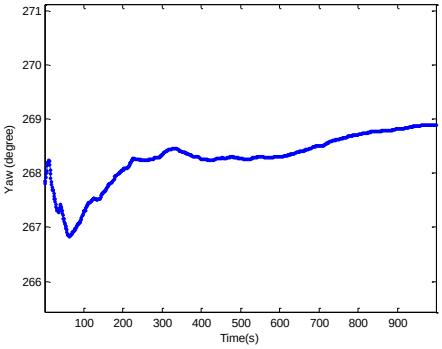

Fig.10 The yaw results of the UAV test

As is shown, the resolved yaw is consistent with true moving direction. The fluctuation range is between 265.5 degree and 271.1 degree.

C. Accuracy Assessment of Heading Angle

Note that, the heading determination of GPS compass is not dependent on the velocity and the Earth's magnetic field. To evaluate the accuracy better, four static experiments are performed, in which the baseline is set up pointing to north, east, south and west, respectively. As shown in Table I, the average and standard deviation of heading and pitch angle measurements are given (without Kalman filter).

TABLE I. HEADING ACCURACY ASSESSMENT

Baseline Placement	Mean Value (degree)	Standard deviation (degree)
North	0.0088	0.7782
East	90.5425	0.7125
South	179.5269	0.7458
West	269.8588	0.7045

Since the mean values of those four static experiments are close to the true baseline placement, the correctness of the prototype system is thus be verified. With the standard deviation of the heading angle, it can also be inferred that the yaw accuracy of prototype system is about 0.7° and this is reasonable for a 0.4m baseline.

With the actual dynamic and static experimental results above, the correctness of GPS compass can be proved based on the six-rotor UAV platform.

V. ACKNOWLEDGEMENTS

This work is supported by the Undergraduate Training Programs for Innovation and Entrepreneurship of Civil Aviation University of China (Grant No.IECAUC2016132)

REFERENCES

[1] A.D King "Inertial Navigation – Forty Years of Evolution". GEC Review, vol. 13, pp.140-149, March 1998.

[2] C.H. Tu, K.Y Tu, F.R. Chang and L.S. Wang, "GPS compass: a novel navigation equipment," IEEE Trans Aerosp Electron Sys, vol. 33, pp. 1063–1068, July 1996.

[3] A. Leick, GPS satellite surveying, 3rd ed., Wiley, New York, 2004, pp.324-337.

[4] P.J.G Teunissen, "Integer least squares theory for the GNSS Compass," Journal of Geodesy, vol. 83, pp. 1-15, January 2010.

[5] P.J. Buist, "The Baseline Constrained LAMBDA Method for Single Epoch, Single Frequency Attitude Determination Applications", Proceedings of ION-GPS, Forth Worth, Texas, USA, 2007.

[6] P.J.G Teunissen, "The LAMBDA method for the GNSS compass," Artif. Satellites, vol. 41, pp. 89-105, July 2007.

[7] C. Park, P.J.G Teunissen, "Integer least squares with quadratic equality constraints and its application to GNSS attitude determination systems," Int J Control Autom Syst, vol.7, pp. 566-576, December 2009.

[8] P.J.G Teunissen, G. Giorgi, P.J Buist, "Testing of a new single-frequency GNSS carrier-phase compass method: land, ship and aircraft experiments," GPS Solutions, vol. 15, pp. 15-28, January 2011.

[9] W. Chen, H. Qin, Y. Zhang, T. Jin, "Accuracy assessment of single and double difference models for the single epoch GPS compass", Advances in Space Research, vol. 49, pp. 725-738, Decemeber 2012.